Iron stores and Cerebral Veins in MS Studied by Susceptibility Weighted Imaging (SWI)

E. Mark Haacke[a], James Garbern[a], Yanwei Miao[b], Charbel Habib[a], Manju Liu[a].

[a]Department of Radiology, Wayne State University, Detroit, MI 48202, USA

[b]Department of Radiology, the First Affiliated Hospital, Dalian Medical University, Dalian, Liaoning 116011, China

Corresponding Author:

E. Mark Haacke, PhD
Wayne State University
MR Research Facility
Department of Radiology
HUH—MR Research G030/Radiology
3990 John R Road
Detroit, MI 48201
Tel. (313) 745-1395
Fax (313) 745-9182
Email: nmrimaging@aol.com

Abstract

Aim: Multiple sclerosis (MS) is a disease whose etiology until recently has remained a mystery. A possible explanation for MS has been put forward by Zamboni et al [1] that it is caused by a chronic cerebrospinal venous insufficiency (CCSVI). In this paper, we show that the iron deposition as seen by susceptibility weighted imaging (SWI) in the basal ganglia and thalamus is consistent with this interpretation.

Methods: 14 MS patients were recruited for this study with a mean age of 38 ranging from 19 to 66 years old. A velocity compensated 3D gradient echo sequence was used to generate susceptibility weighted images (SWI) with a high sensitivity to iron content. We evaluated iron in the following structures: substantia nigra, red nucleus, globus pallidus, putamen, caudate nucleus, thalamus and pulvinar thalamus. Each structure was broken into two parts, a high iron content region and a low iron content region. The measured values were compared to previously established baseline iron content in these structures as a function of age.

Results: Of the 14 cases, 12 revealed an increase in iron above normal levels and with a particular pattern of iron deposition in the medial venous drainage system.

Conclusion: The backward iron accumulation pattern seen in the basal ganglia, thalamus and midbrain of most MS patients is consistent with the hypothesis of venous hypertension.

Key words: brain iron deposition, susceptibility weighted imaging, iron changes in multiple sclerosis

Introduction

It has been suggested recently that multiple sclerosis (MS) may develop as a neurodegenerative disease because of a venous vascular insufficiency [1] and the resulting venous hypertension related directly to abnormalities (narrowing and restricted flow) in the jugular and azygous veins. Although evidence of venous involvement has been known for a long time [2-4], pioneering efforts in this direction have basically been ignored until Zamboni et al [1] demonstrated the presence of stenoses in MS patients. This is truly a paradigm shift, where one must look outside the brain, in this case the cardiovascular system, to understand the source of the brain's problem in MS. Evidently, the venous hypertension that leads to multiple sclerosis can have a damaging effect on the vessel wall [5,6]. This is best understood from research related to chronic venous disease where it has been shown that changes in venous hemodynamics leads to a disruption of flow, a reduction of the shear stress in the vessel wall, an inflammatory degenerative response and, subsequently, a deterioration of the venous wall [7-9]. Similar effects are known in atherosclerosis when normal flow is disrupted. And even in multiple sclerosis research dating back to the work of Adams [2], and later Trojano [10], venous wall breakdown in multiple sclerosis has been well documented.

Following this argument a bit further, one might expect then local iron increases from the damaged vessel wall, loss of vessel function, reduced transit times and reduced local blood flow in the chronic stages of the disease. One might also expect that the vascular pathways most closely associated with the hypertension and local reflux (especially in the areas of the internal cerebral veins and vein of Galen) associated with obstructed venous flow would in turn lead to local venous damage in multiple sclerosis [11-13]. The areas most affected by this might well be the thalamus and basal ganglia since they are associated with the medial venous drainage system [14].

With this philosophy in mind, we investigated the local iron content in the basal ganglia and thalamus using susceptibility weighted imaging (SWI) to see if there were any evidence of such microbleeding or vascular breakdown that followed a pathway reverse to that of the draining veins as noted by Fog in 1964 [3] and later espoused by Schelling [4].

SWI is a gradient echo MR imaging technique that uses phase as an alternate source of information to enhance contrast [15]. It uses the susceptibility differences between tissues to generate this contrast. Susceptibility is very different than the usual spin density, T1 and T2 properties. It is represented indirectly by the phase images and in this case by the SWI filtered phase images that are used to remove background field inhomogeneities. These phase images produce the same image, whether acquired at 1.5T, 3T or any other field strength as long as the product of B_oTE is a constant. Thus, while other tissue properties change from field strength to field strength, phase properly adjusted for TE will not. That is because susceptibility does not change from one field strength to another. The early applications of SWI stemmed from the signal changes that took place in the SWI images for veins [16]. The presence of deoxygenated blood leads to both a T2* effect and a change in phase in the veins since deoxyhemoglobin is paramagnetic. Combining these two characteristics into SWI data led to a beautiful perspective of the venous system in the brain. Similar to how the blood oxygenation level dependent (BOLD) effect is used in functional brain imaging, SWI shows veins with less deoxyhemoglobin as less suppressed and those with more deoxyhemoglobin as more suppressed. Several examples of the venograms that are possible with SWI at 3T are shown in Figure 1. In this paper, our interest is to combine the venous vascular information in SWI processed data with the putative iron content seen in SWI high pass filtered phase data. These two pieces of information can then

be used to assess the state of the venous vasculature in multiple sclerosis patients. Some example SWI filtered phase images good for visualizing iron are shown in Figure 2.

To this end, we compared the iron in a series of 14 multiple sclerosis patients with that in a set of 100 normal subjects using SWI. Our goal was to look for iron abnormalities and evaluate whether these could be integrated into this new theory of cerebral spinal venous insufficiency.

Materials and Methods

Fourteen (14) clinically defined MS patients were imaged with mean age of 38 ranging from 19 to 66 years old. All patients signed a consent form approved by the Internal Review Board (IRB-approved). A velocity compensated 3D gradient echo sequence was used to generate susceptibility weighted images (SWI) with a high sensitivity to iron content. All SWI images were acquired at 1.5T Sonata [Siemens, Erlangen, Germany] with a resolution of $0.5x0.5x2mm^3$. Imaging parameters were TR=57ms, TE=40ms; FA=20°; and BW=80 Hz/pixel. A 64x64 low spatial frequency kernel was used to complex-divide into the original data to create an effective high pass filtered phase image. The resulting SWI filtered phase images were used as a means to quantify iron content *in vivo*. The following 7 deep gray matter structures were studied for iron content including: the globus pallidus (GP), the caudate nucleus (CN), the putamen (PUT), the thalamus (THA), the substantia nigra (SN), the red nucleus (RN) and the pulvinar thalamus (PT).

A two region analysis concept was used where each structure was separated into two regions-of-interest (ROI): the normal iron content region (RI) and the high iron content region (RII). These regions were differentiated using threshold values cited in previous work by Haacke et al. in 2007 [17]. The measured values were compared to a previously established baseline of iron content

in these structures as a function of age. This process has also been described in more detail in Haacke et al (JMRI, in press). In this work, we considered the different measures of iron in the high iron content region (RII): the area of the high iron content region (percentage), the average iron per voxel in the high iron content region, the total and the average iron in each structure.

In order to make these results available for comparison with other papers, Haacke et al [17] suggested that one could correlate the measured phase changes μg Fe/g tissue [17,18]. Moreover, phase changes can also be expressed in terms of parts per million (ppm) and radians. The conversion factors between these units are provided below for a left handed system (for a right handed system $\Delta\varphi$ becomes $-\Delta\varphi$):

from Siemens phase units (SPU) to radians:

$$\Delta\varphi \text{ (radians)} = (\varphi_{SPU}-2048)\pi/2048 \quad (1)$$

from δ ppm to radians:

$$\Delta\varphi(\text{radians}) = 5.09\pi\delta \quad (2)$$

from SPU to μg iron:

$$[Fe] = (\Delta\varphi_{SPU}/180)(60\mu g/cc)(\text{pixel number})(\text{pixel volume}) \quad (3)$$

Equation 3 is derived by taking 180 SPU to be equivalent to 60 μg Fe/g tissue [18]. However, T2* changes as a function of iron concentration suggest that a phase change of 180 SPU (0.276 radians) could represent as much as 240 μg Fe/g fresh tissue. If this number were used, then the amount of iron would be 4 times higher than what we quote here.

Results

In order to appreciate the changes in iron content that occur for different regions of the brain, we show in Figure 3 a normal volunteer/multiple sclerosis patient comparison for the thalamostriate area (A,B) and the midbrain (C,D). The young normal volunteer (age 32) shows little iron build up in the basal ganglia or thalamus (A) while the MS patient shows high iron content especially in the right hand globus pallidus (B). A different subject (C)/patient (D) comparison is shown for the midbrain in Figures 3C,D. Here, the MS patient shows high iron content in both the left and right substantia nigra.

Comparing MS to controls quantitatively, iron changes as a function of age revealed different results for different structures and showed variability while considering different parameters (total iron, average iron and area). However, our results revealed that 85% of the patients showed a significant increase in iron compared to controls in at least one of the studied structures. This percentage showed some variation while considering total iron versus average iron. For instance, evaluating total iron content in the whole structure showed that 50% of the studied group has abnormal iron, while 71.4% of these patients were evaluated as having abnormal iron content when studying the average iron content per pixel. Using the two region analysis concept, 64%, 79% and 85% of the studied group showed abnormal iron deposition when evaluating total, average and area of iron content in RII respectively.

In brief, the results of using different parameters to evaluate iron content are shown in Table 1. These results demonstrate that evaluating abnormal iron content is not best achieved by using total iron content measurements rather more information can be gleaned by evaluating the area of

the high iron content region (RII) as well as the average iron per pixel. These latter two measures appear to present better quantitative indicators of iron content abnormality.

The results of this study also show that iron abnormalities may be found in different structures if we consider different ages. For instance, iron overload in the pulvinar thalamus is shown to be dominant in young people (19 to 35 years), whereas abnormal iron in the substantia nigra is shown to be dominant for middle age (35 to 50 years). This dominance for the PT and SN was well seen in all of total iron, average iron and area. By taking each parameter separately, studying total and average iron content in the whole region shows that the abnormality is mostly seen in the SN. On the other hand, total and average iron content in the high iron region shows that the abnormality is equally seen in the PT and the SN. However, evaluating the area of iron in RII showed dominance in the PT and the THA. Note that iron abnormality in the latter was very low and even absent in evaluating the whole region and total iron content.

Two representative plots are shown here to demonstrate the high iron content regions for the pulvinar thalamus and the substantia nigra (Figure 4). Clearly, many of the younger people with MS have a higher iron content than normal young people.

Discussion

The interest and association of MS with veins dates back to at Putnam in 1937 [19] and later Fog [3] in 1964 with a major decade's long effort to convince people of the role of the mechanical effects of changes in venous flow by Schelling [4]. However, the excitement comes from a proof of concept that MS is a chronic cerebral spinal venous insufficiency by Paolo Zamboni and his team [1]. This exciting work, done with ultrasound and followed by a corrective surgical procedure, shows that the etiology of MS may be venous stenoses and the subsequent damage from abnormal flow patterns to the venous system. That is, MS is a perivenular disease first and an inflammatory demyelinating disease second. In fact, CCSVI provides a logical explanation as to why the entire brain is affected in MS, why the disease tracks backward along the venous drainage system, and why it emanates from the white matter near the ventricles in the drainage territory of the medullary veins. We know that the basal ganglia from the dentate nucleus, the midbrain and up to the thalamostriate system are all drained by the medial venous drainage system out the straight sinus. It is just these regions that have increased iron content as seen with SWI and with conventional MRI when one reviews the literature [6,14,20-24]. It appears then that these increases in iron may represent venous endothelial damage as a consequence of CCSVI.

Brain iron accumulation has been shown histologically in neurodegeneration diseases including MS [25,26]. Moreover, some studies using experimental autoimmune encephalomyelitis animal models to understand the pathogenesis of MS showed excessive iron deposition and abnormal brain iron metabolism [27,28]. One explanation for this overload is that iron accumulates through a cyclic inflammatory process. During this mechanism, inflammation attracts iron-rich macrophages, whose presence increases the local iron content. This iron accumulation leads to

further inflammation and iron deposition, causing the system to be self-sustainable [29]. Another source of excessive brain iron in MS patients has been assumed to be from myelin or oligodendrocyte debris [27], concentrated iron in the macrophages, or as a product of local microhemorrhages following venous or venule wall damage [2,30,31]. As the wall breaks down, free iron may escape outside the vessel. Free iron is known to cause the formation of highly reactive hydroxyl radicals that can trigger cell membrane dysfunction and chronic microglial activation [29]. However, it is still unknown whether iron deposition is a cause or a consequence of the inflammatory demyelinating aspect in MS pathology.

Recently, the work by Bakshi et al [14] showed the presence of deep gray matter T2 hypointensities and suggested that excessive iron deposition is associated with the progression of disease. This effect was seen in the caudate nucleus, the putamen and the thalamus, and correlated with patients' clinical outcomes. These observations on iron content are in agreement with our own work presented in this paper.

On the other hand, recent MR SWI studies have used phase information to evaluate iron content as a function of age in the human brain [32-34]. These papers did not consider breaking the structures into low and high iron content regions. In this work, we introduced the concept of a high iron content region and normal iron content region. This made it possible to study not only smaller increases in iron content more confidently but also to study both the average iron content per pixel and the area of increased iron content with age which showed different and interesting results as mentioned earlier. This approach revealed subtle changes in iron content that cannot be seen with the single region approach.

The iron load seen in the basal ganglia, the thalamus and the midbrain is consistent with the hypothesis of venous hypertension. All of these structures (including the dentate nucleus which we did not analyze) have veins that eventually drain out the straight sinus. Recently, even the dentate nucleus has been shown to have an increase in iron content for MS patients [35,36]. It may be no surprise then that one or many of these structures eventually suffers if there is a chronic venous hypertension. Predicting which of these structures breaks down first or why these effects can be bilateral or unilateral remains to be investigated. If the balloon angioplasty treatment stops the progression of MS, then perhaps SWI can be used to monitor any further changes of iron.

Conclusion

In summary, SWI phase data provide a new approach to measuring brain iron as a function of age. When a two compartment model (low iron versus high iron dominant region) is used, significant changes in iron content as a function of age are seen. By assessing the changes in iron content with SWI, it may be possible to monitor the worsening or improvements in the vascular situation at least with respect to the iron component. Whether or not the brain is able to clear away such iron depositions over time after treatment is unknown at this time. Further work will need to be done to monitor iron in MS patients whether they undergo balloon angioplasty for CCSVI or not. In this sense, iron may serve as a biomarker for at least the vascular portion of MS disease.

References

1. Zamboni P, Galeotti R, Menegatti E, Malagoni AM, Tacconi G, Dall'Ara S, et al. Chronic cerebrospinal venous insufficiency in patients with multiple sclerosis. J Neurol Neurosurg Psychiatry 2009;80:392-9.
2. Adams CW. Perivascular iron deposition and other vascular damage in multiple sclerosis. J Neurol Neurosurg Psychiatry 1988;51:260-5.
3. Fog T. On the Vessel-Plaque Relationships in the Brain in Multiple Sclerosis. Acta Neurol Scand Suppl 1964;40:SUPPL 10:9-5.
4. Schelling F. Damaging venous reflux into the skull or spine: relevance to multiple sclerosis. Med Hypotheses 1986;21:141-8.
5. Zamboni P. The big idea: iron-dependent inflammation in venous disease and proposed parallels in multiple sclerosis. J R Soc Med 2006;99:589-93.
6. Singh AV, Zamboni P. Anomalous venous blood flow and iron deposition in multiple sclerosis. J Cereb Blood Flow Metab 2009.
7. Bergan JJ, Pascarella L, Schmid-Schonbein GW. Pathogenesis of primary chronic venous disease: Insights from animal models of venous hypertension. J Vasc Surg 2008;47:183-92.
8. Bergan JJ, Schmid-Schonbein GW, Smith PD, Nicolaides AN, Boisseau MR, Eklof B. Chronic venous disease. N Engl J Med 2006;355:488-98.
9. Zamboni P, Menegatti E, Bartolomei I, Galeotti R, Malagoni AM, Tacconi G, et al. Intracranial venous haemodynamics in multiple sclerosis. Curr Neurovasc Res 2007;4:252-8.
10. Trojano M, Manzari C, Livrea P. Blood-brain barrier changes in multiple sclerosis. Ital J Neurol Sci 1992;13:55-64.
11. Ge Y, Zohrabian VM, Osa EO, Xu J, Jaggi H, Herbert J, et al. Diminished visibility of cerebral venous vasculature in multiple sclerosis by susceptibility-weighted imaging at 3.0 Tesla. J Magn Reson Imaging 2009;29:1190-4.
12. Law M, Saindane AM, Ge Y, Babb JS, Johnson G, Mannon LJ, et al. Microvascular abnormality in relapsing-remitting multiple sclerosis: perfusion MR imaging findings in normal-appearing white matter. Radiology 2004;231:645-52.
13. Wuerfel J, Bellmann-Strobl J, Brunecker P, Aktas O, McFarland H, Villringer A, et al. Changes in cerebral perfusion precede plaque formation in multiple sclerosis: a longitudinal perfusion MRI study. Brain 2004;127:111-9.
14. Neema M, Arora A, Healy BC, Guss ZD, Brass SD, Duan Y, et al. Deep gray matter involvement on brain MRI scans is associated with clinical progression in multiple sclerosis. J Neuroimaging 2009;19:3-8.
15. Haacke EM, Mittal S, Wu Z, Neelavalli J, Cheng YC. Susceptibility-weighted imaging: technical aspects and clinical applications, part 1. AJNR Am J Neuroradiol 2009;30:19-30.
16. Reichenbach JR, Venkatesan R, Schillinger DJ, Kido DK, Haacke EM. Small vessels in the human brain: MR venography with deoxyhemoglobin as an intrinsic contrast agent. Radiology 1997;204:272-7.
17. Haacke EM, Ayaz M, Khan A, Manova ES, Krishnamurthy B, Gollapalli L, et al. Establishing a baseline phase behavior in magnetic resonance imaging to determine normal vs. abnormal iron content in the brain. J Magn Reson Imaging 2007;26:256-64.
18. Haacke EM, Cheng NY, House MJ, Liu Q, Neelavalli J, Ogg RJ, et al. Imaging iron stores in the brain using magnetic resonance imaging. Magn Reson Imaging 2005;23:1-25.

19. Putnam TJ, Adler A. MS plaques spread along the periventricular veins. Arch of Neurology and Psychiatry 1937;38:1-15.
20. Bakshi R, Benedict RH, Bermel RA, Caruthers SD, Puli SR, Tjoa CW, et al. T2 hypointensity in the deep gray matter of patients with multiple sclerosis: a quantitative magnetic resonance imaging study. Arch Neurol 2002;59:62-8.
21. Drayer B, Burger P, Hurwitz B, Dawson D, Cain J. Reduced signal intensity on MR images of thalamus and putamen in multiple sclerosis: increased iron content? AJR Am J Roentgenol 1987;149:357-63.
22. Drayer BP, Burger P, Hurwitz B, Dawson D, Cain J, Leong J, et al. Magnetic resonance imaging in multiple sclerosis: decreased signal in thalamus and putamen. Ann Neurol 1987;22:546-50.
23. Khalil M, Enzinger C, Langkammer C, Tscherner M, Wallner-Blazek M, Jehna M, et al. Quantitative assessment of brain iron by R(2)* relaxometry in patients with clinically isolated syndrome and relapsing-remitting multiple sclerosis. Mult Scler 2009;15:1048-54.
24. Walter U, Wagner S, Horowski S, Benecke R, Zettl UK. Transcranial brain sonography findings predict disease progression in multiple sclerosis. Neurology 2009;73:1010-7.
25. Craelius W, Migdal MW, Luessenhop CP, Sugar A, Mihalakis I. Iron deposits surrounding multiple sclerosis plaques. Arch Pathol Lab Med 1982;106:397-9.
26. Levine SM, Chakrabarty A. The role of iron in the pathogenesis of experimental allergic encephalomyelitis and multiple sclerosis. Ann N Y Acad Sci 2004;1012:252-66.
27. Forge JK, Pedchenko TV, LeVine SM. Iron deposits in the central nervous system of SJL mice with experimental allergic encephalomyelitis. Life Sci 1998;63:2271-84.
28. Pedchenko TV, LeVine SM. Desferrioxamine suppresses experimental allergic encephalomyelitis induced by MBP in SJL mice. J Neuroimmunol 1998;84:188-97.
29. Hammond KE, Metcalf M, Carvajal L, Okuda DT, Srinivasan R, Vigneron D, et al. Quantitative in vivo magnetic resonance imaging of multiple sclerosis at 7 Tesla with sensitivity to iron. Ann Neurol 2008;64:707-13.
30. Schenck JF, Zimmerman EA. High-field magnetic resonance imaging of brain iron: birth of a biomarker? NMR Biomed 2004;17:433-45.
31. Walton JC, Kaufmann JC. Iron deposits and multiple sclerosis. Arch Pathol Lab Med 1984;108:755-6.
32. Ogg RJ, Langston JW, Haacke EM, Steen RG, Taylor JS. The correlation between phase shifts in gradient-echo MR images and regional brain iron concentration. Magn Reson Imaging 1999;17:1141-8.
33. Wismer GL, Buxton RB, Rosen BR, Fisel CR, Oot RF, Brady TJ, et al. Susceptibility induced MR line broadening: applications to brain iron mapping. J Comput Assist Tomogr 1988;12:259-65.
34. Xu X, Wang Q, Zhang M. Age, gender, and hemispheric differences in iron deposition in the human brain: an in vivo MRI study. Neuroimage 2008;40:35-42.
35. Roccatagliata L, Vuolo L, Bonzano L, Pichiecchio A, Mancardi GL. Multiple sclerosis: hyperintense dentate nucleus on unenhanced T1-weighted MR images is associated with the secondary progressive subtype. Radiology 2009;251:503-10.
36. Tjoa CW, Benedict RH, Weinstock-Guttman B, Fabiano AJ, Bakshi R. MRI T2 hypointensity of the dentate nucleus is related to ambulatory impairment in multiple sclerosis. J Neurol Sci 2005;234:17-24.

Figure legends

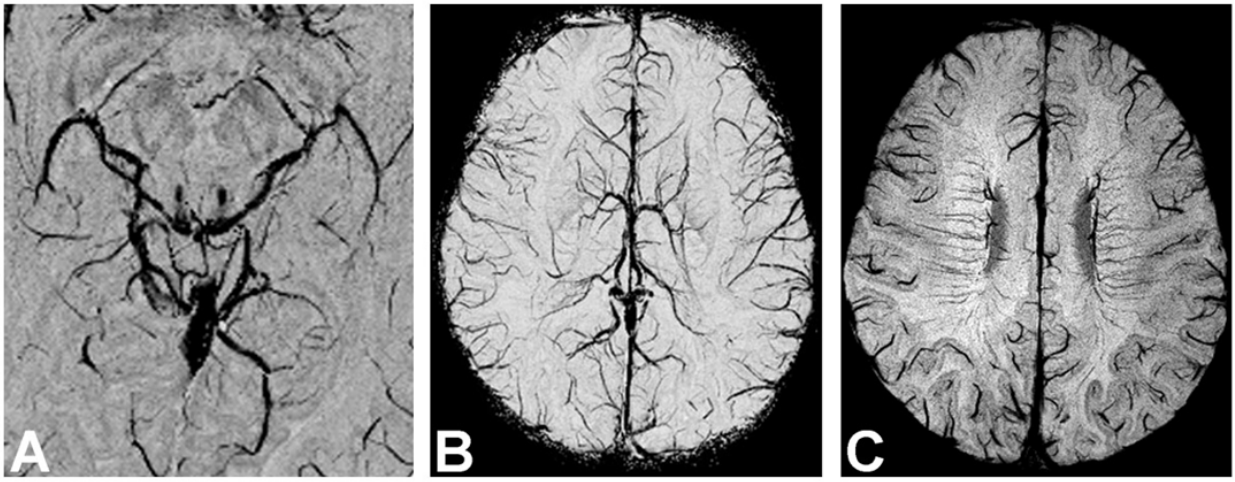

Figure 1: Images acquired at 3T with 0.5mm x 0.5mm x 2mm resolution. Each mIP is over 10 slices or an equivalent slab that is 2cm thick. (A) midbrain, (B) thalamostriate region and (C) the medullary veins.

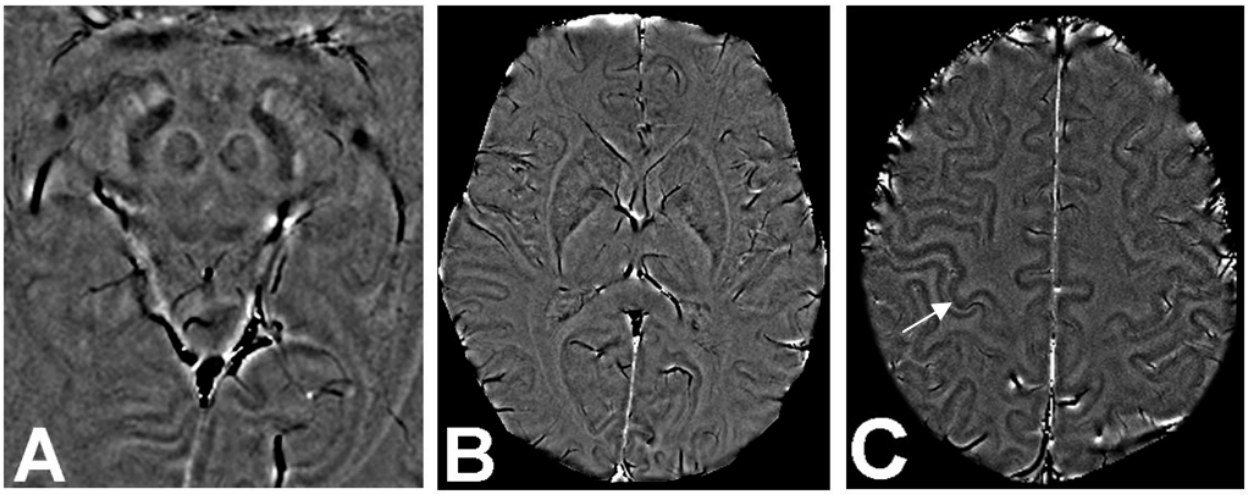

Figure 2: Example phase images in a normal young volunteer through (a) the midbrain, (b) the thalamostriate area, and (c) the upper brain showing the motor cortex (arrow).

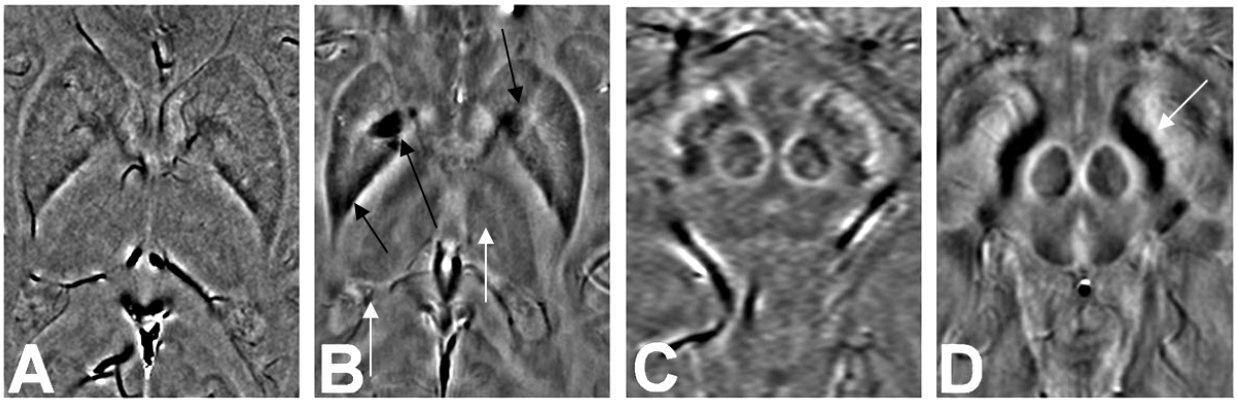

Figure 3: Here, we show some example phase images for an age matched normal control (A, C) and an MS patient (B,D) for the basal ganglia and thalamus (A and B) and the midbrain (C and D). Note the heavy iron deposition (arrows): in the lower part of the caudate as well as in the globus pallidus and at the boundaries of the putamen (B, black arrows). Also, iron content has increased in the thalamus (and pulvinar thalamus B, white arrows) and in the substantia nigra (D, white arrow).

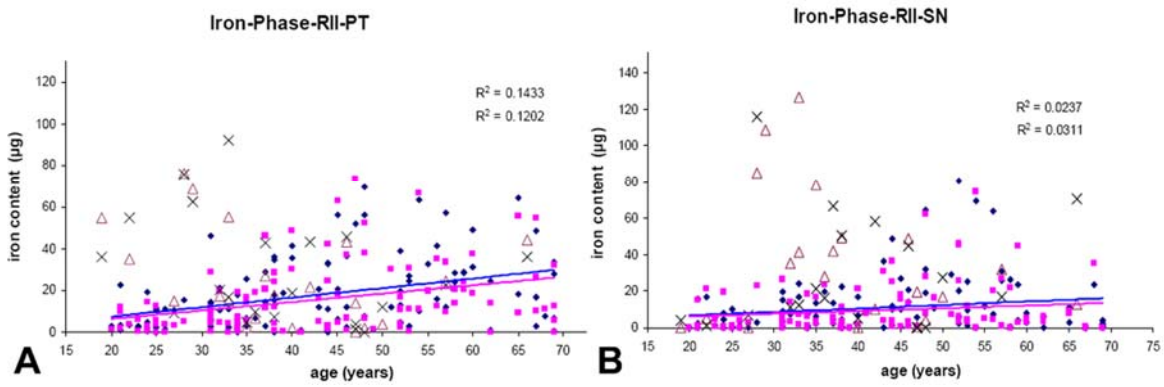

Figure 4: Iron content as a function of age for: A) the pulvinar thalamus and B) the substantia nigra. The squares and the dots represent the iron values measured in region II using phase information, in the left and right hemispheres respectively, and the lines represent their linear regression. The crosses and the triangles represent the iron values in the left and right hemisphere of the studied 14 MS patients respectively.

Tables

Table 1. Number of MS patients revealing abnormal iron content in each structure for different parameters. Counting all structures, 12 of 14 patients had at least one structure with abnormally high iron content.

Parameters	CN	GP	PUT	PT	RN	SN	THA
WS-AI	2	3	1	5	2	8	0
WS-TI	2	2	2	4	2	4	0
RII-TA	3	4	2	6	4	6	0
RII-TI	3	2	3	6	1	6	1
RII-AI	4	4	3	7	5	4	7
All regions	6	6	5	7	6	8	7

Note: WS-AI: Whole Structure - Average Iron; WS-TI: Whole Structure - Total Iron; RII-TA: Region II - Total Area; RII-TI: Region II - Total Iron; RII-AI: Region II - Average Iron